Temperature Jump-Induced Secondary Structural Change of the Membrane Protein Bacteriorhodopsin in the Premelting Temperature Region: A Nanosecond Time-Resolved Fourier Transform Infrared Study

Jianping Wang and Mostafa A. El-Sayed

Laser Dynamic Laboratory, School of Chemistry and Biochemistry, Georgia Institute of Technology, Atlanta, Georgia 30332-0400 USA

ABSTRACT   The secondary structural changes of the membrane protein, bacteriorhodopsin, are studied during the premelting reversible transition by using laser-induced temperature jump technique and nanosecond time-resolved Fourier transform infrared spectroscopy. The helical structural changes are triggered by using a 15°C temperature jump induced from a preheated bacteriorhodopsin in D_2O solution at a temperature of 72°C. The structural transition from α_{II}- to α_I-helices is observed by following the change in the frequency of the amide I band from 1667 to 1651 cm^{-1} and the shift in the frequency of the amide II vibration from 1542 cm^{-1} to 1436 cm^{-1} upon H/D exchange. It is found that although the amide I band changes its frequency on a time scale of <100 ns, the H/D exchange shifts the frequency of the amide II band and causes a complex changes in the 1651–1600 cm^{-1} and 1530–1430 cm^{-1} frequency region on a longer time scale (>300 ns). Our result suggests that in this "premelting transition" temperature region of bacteriorhodopsin, an intrahelical conformation conversion of the α_{II} to α_I leads to the exposure of the hydrophobic region of the protein to the aqueous medium.

INTRODUCTION

Bacteriorhodopsin (bR) is the protein found in the cytoplasmic membrane of *Halobacterium salinarium* (Oesterhelt and Stoeckenius, 1974). The purple membrane (PM) consists of a two-dimensional, hexagonal lattice of protein trimer structure that organizes the individual bR molecules. It has only one polypeptide chain of 248 amino acid residues with known sequence (Henderson et al., 1990) and a retinal chromophore that binds to the ϵ-amino group Lys-216 through a protonated Schiff base. The secondary structure of bR is well characterized with a peptide sequence that traverses the membrane seven times in the form of α-helices (Henderson et al., 1990). The photochemistry of bR has been extensively studied in the past decades (Birge, 1990; Mathies et al., 1991; Lanyi, 1993; Ebrey, 1993). Upon absorbing light, bR undergoes a photocycle and pumps a proton across its membrane, creating an electrochemical proton gradient. The electrochemical energy resulting from the proton gradient is used for the synthesis of adenosine 5′-triphosophate.

It has been proposed by Krimm and Dwivedi (1982) that the bR transmembrane helices are α_{II}-helical in nature, in contrast to the normal α_I-helical structure found in polypeptides and proteins. In the α_{II}-helical structure, the ϕ and ψ dihedral angles are different from those in α_I-helical conformation, leading to an outward projections of the C=O groups from the helix axis accompanied by an inward tilting of the N-H groups. In α_{II}-helical structure, the H-bond

length is slightly longer than that in α_I. Vibrational normal mode analysis for polyalanine (Krimm and Dwivedi, 1982) predicts significant frequency differences between the standard α_I- and the modified α_{II}-helical conformation. This results in an increase of ~10 cm^{-1} in the amide I mode at 1658 cm^{-1} (essentially C=O stretching) in α_{II}-helical structure (Krimm and Dwivedi, 1982). Indeed, infrared spectroscopic studies of bR substantiate the appearance of a high frequency amide I mode at 1667 cm^{-1}. A number of other spectroscopic data also strongly support the existence of α_{II}-helices in bR, e.g., Raman (Vogel and Gartner, 1987), ultraviolet-circular dichroism (UV-CD) (Gibson and Cassim, 1989), and ^{13}C-nuclear magnetic resonance study (Tuzi et al., 1994). In addition, it has been suggested that the infrared band at 1665 cm^{-1} shows up only when bR monomers interact with each other to form trimers (Torres et al., 1995).

Aqueous bR is susceptible to thermal denaturation. The melting temperature (T_m) of native bR is $\sim96°C$. Differential scanning calorimetry (DSC) experiments show the presence of two thermal transitions for native purple membrane (Jackson and Sturtevant, 1978; Brouillette et al., 1987; Cladera et al., 1988), a small transition centered at $\sim80°C$ and a main transition at $\sim96°C$. The 80°C transition is found to be highly reversible, whereas the main transition appears to be irreversible (Jackson and Sturtevant, 1978). The reversible transition is associated with a cooperative disordering of the paracrystalline lattice distribution of bR molecules (Jackson and Sturtevant, 1978; Hiraki et al., 1981). By using an annealing procedure (Shnyrov and Mateo, 1993), up to five successive thermal transitions are reported in the temperature range of 60–105°C, among which only the transition at $\sim72°C$ is reported to be reversible. Kresheck et al. (1990) have studied the thermal stability of native, delipidated, deionized, and Mg^{2+} regenerated

bR by DSC and circular dichroism (CD) spectroscopy. All these perturbations were shown to lower the T_m, except in the case when bR is delipidated. However, the influence on the thermal stability is less significant than that on the proton pumping efficiency. It is also found that adding Mg^{2+} to deionized bR does not restore the thermal stability of native bR, although it restores the photocycle of bR (Kresheck et al., 1990). A given pathway of thermal denaturation of bR in D_2O has been suggested based on the results of a Fourier transform infrared spectroscopy (FTIR) study (Taneva et al., 1995). These authors conclude that the thermal denaturation of bR is a kinetically controlled process.

Understanding the folding mechanism of a protein is very important to determine the connection, if any, between the biochemical synthesis of the protein and the variety of its biological functions. How the secondary and tertiary structures of proteins are formed from the nonnative conformational state is still not fully understood. In addition, the unfolding processes, especially the fast events (shorter than 10 ms), are drawing much attention recently. Laser T-jump (Phillips et al., 1995; Ballew et al., 1996; Williams et al., 1996) is one of the useful techniques to initiate the fast secondary structure change. Time-resolved fluorescence, single wavelength time-resolved IR as well as other techniques have been used as dynamic approaches to follow secondary or tertiary conformational changes in proteins. Refolding of cold denatured apomyoglobin by laser T-jump has uncovered 250 ns to 5 μs kinetics associated with secondary structure and core formation (Ballew et al., 1996); the helix-coil transition in the peptide suc-21 exhibits a time constant of $\sim$160 ns and a few milliseconds relaxation to the initial condition as the temperature in the medium decays after the jump (Williams et al., 1996).

FTIR spectroscopy is one of the most powerful techniques to obtain information about the secondary structure of a protein. In addition, time-resolved techniques are useful in gaining insight into the dynamics of protein unfolding and folding. By using time-resolved FTIR spectroscopy, the dynamical conformational changes occurring during these fast events can be obtained. In the present study, the fast structural changes are initiated by a short infrared laser pulse that generates a transient rise in temperature of up to 15°C. The step-scan time-resolved FTIR technique is used to follow the protein conformational change in the spectral region of amide I and amide II modes. It is found that the T-jump-induced protein secondary structural transition from α_{II}- to α_I-helices, occurs in the nanosecond time domain. The recovery process from α_I to α_{II} structure occurs within a few milliseconds as a direct or indirect result of the temperature relaxation after the T-jump.

MATERIALS AND METHODS

Sample

Purple membrane was isolated from the *H. salinarium* strain ET1001 as described previously (Oesterhelt and Stoeckenius, 1974). Membrane sus-

pension in D_2O was prepared by washing the membrane 6–8 times with D_2O through the centrifugation-resuspension cycle and was handled under an argon atmosphere to eliminate contamination from humid air. The initial pH of the concentrated suspension before D_2O exchange was typically 6.8. A 50-μm path-length IR cell with two CaF_2 plates and a Teflon spacer was used for bR. Samples with $OD_{568 nm} = 0.8$ in the IR cell were studied as a function of temperature in the range of 30–97°C by using a thermostated bath system (RET-100, NESLAB Instruments, Inc., Union City, CA). After the desired temperature was stabilized, the steady-state spectrum was taken as the average of 100 scans at a resolution 2 cm^{-1}. A melting curve was obtained by plotting the absorbance change in the amide I band at 1667 cm^{-1} as a function temperature.

T-jump apparatus

The 1064-nm output of a Nd-YAG laser (YAG 660, Quantel International, Santa Clara, CA) was focused into a Raman cell (stainless steel tube with quartz windows, 85-cm length and 32-mm diameter, filled with 160 psi H_2). This produced the heating pulse at 1.9 μm (10-ns pulse width, 2–10 mJ/pulse at 5 Hz) for the T-jump experiment. This heating pulse was absorbed by the overtone of the O-D stretching vibration in D_2O, a weak absorption centered at $\sim$5500 cm^{-1} ($\epsilon = 10$ cm^{-1}). The sample heating volume was $\sim$2 $mm^2 \times 50$ μm. This resulted in a T-jump of $\Delta T = T - T_0 = 15°C$ at $T_0 = 72°C$.

Time-resolved FTIR spectroscopy

The step-scan FTIR system was an IFS 66/S system (Bruker, Billerica, MA). An MCT detector with a 10-ns response time was used. The ac-coupled signal was amplified by a factor of 125 before inputting it to a 200-MHz digitizer. The dc output of the detector was first adjusted to remove the offset and then amplified to approach $\pm$1-V peak to peak amplitude before introducing it to the digitizer. Fourier transform of the ac-coupled signal used the phase obtained from the dc-coupled signal for phase correction. The time-resolved FTIR spectrum for a certain time domain was calculated based on the dc and ac coupled single channel spectra: $\Delta Abs = Log_{10}(ac/dc + 1)$. An anti-reflecting-coated germanium band-pass filter was used to give a narrow spectrum window of 750-2000 cm^{-1}. Ten to 15 coadditions were used for better signal/noise ratio. In the present study, data were taken with a temporal resolution ranging from 20 ns to 10 μs and a spectral resolution of 4–8 cm^{-1}.

The sample was incubated in the IR cell at 72°C (unless stated otherwise) for various times before exposing it to the 1.9-μm laser heating beam. Static FTIR spectra and UV/Vis spectra were taken before and after the experiment with no significant optical density change in bR observed after the T-jump experiment.

RESULTS

Static FTIR study on bR in D_2O

In order to monitor the thermal-induced structure changes of bR under thermodynamic control and to aid the interpretation of the time-resolved FTIR spectra, static FTIR spectra were measured in the 30–97°C temperature range. Fig. 1 gives the FTIR spectra of concentrated bR in D_2O at different temperatures (from 72–97°C, as indicated by arrows) in the spectral region of 1800 to 1300 cm^{-1}. From Fig. 1 *A*, it can be seen that as the temperature increases, the amide I band shifts from 1667 to 1652 cm^{-1}, whereas the amide II band at 1542 cm^{-1} gradually decreases in intensity, and a broad band around 1436 cm^{-1} increases. The spectral change is shown more clearly in Fig. 1 *B*, in which the
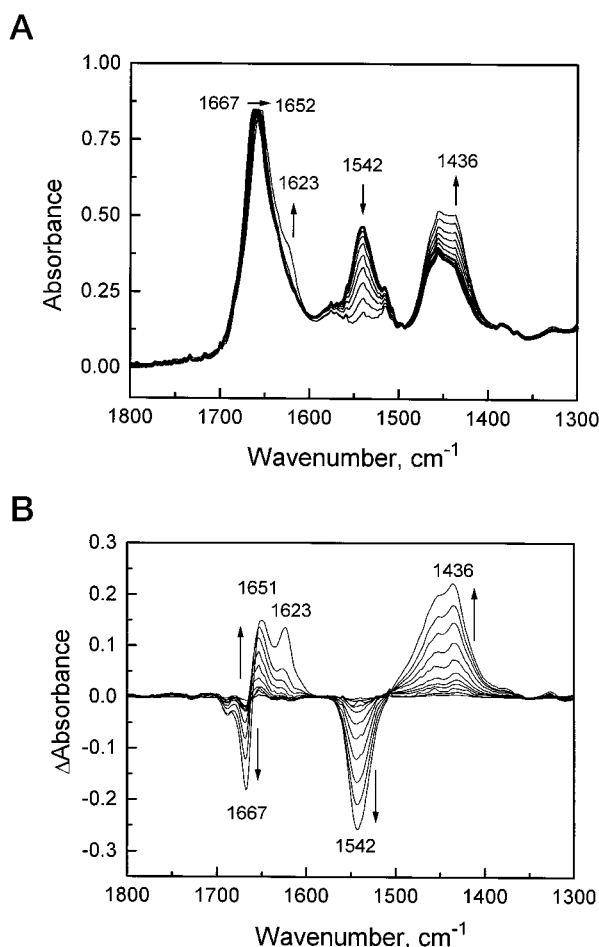
FIGURE 1   (A) FTIR spectra of concentrated bR in D_2O as a function of temperature. The D_2O background has been subtracted at each temperature. The temperature increases along the arrow: 72, 75, 78, 80, 82, 85, 87, 90, 92, 95, 97°C. (B) FTIR difference spectra with the lowest temperature (72°C) spectrum as background. Arrows indicate the absorption change as temperature increases above 72°C.

difference spectra are obtained by subtracting the lowest temperature (72°C) spectrum from spectra at higher temperatures. At higher temperature, two new bands appear at 1651 and 1623 cm^{-1} as the band at 1667 cm^{-1} decreases. There is also a minor band at around 1682 cm^{-1}, overlapping with the negative band at 1667 cm^{-1}. The decrease of the 1542 cm^{-1} band and the increase of the broad band at $\sim$1436 cm^{-1} can be explained as the isotopic substitution of protons with deuterons (from N-H to N-D) (Taneva et al., 1995). In addition, in the course of the temperature change from 72 to 97°C, the band shape, peak position, and relative band area of these difference spectra are temperature-dependent, as shown in Fig. 1 B.

The amide I mode arises predominantly from the collective polypeptide carbonyl C=O stretching vibrations. The negative bands at 1667 and 1542 cm^{-1} are attributed to vibrations of amide I and amide II in the α_{II}–helical structure, respectively. The band assignment is made here according to previous reports (Krimm and Dwivedi, 1982;

Torres et al., 1995). The positive band at 1651 cm^{-1} is assigned to α_I C=O stretching mode because it is located in the region of common α_I-helix (Fraser and MacRae, 1973; Surewicz and Mantsch, 1988). The new band appearing at 1651 cm^{-1} after heating the bR solution has also been reported previously (Cladera et al., 1992; Taneva et al., 1995). The positive band at 1623 cm^{-1} (and 1682 cm^{-1} as well) at high temperature is associated with protein denaturation (Arrondo et al., 1994), resulting from the C=O vibration in the random-coil, a characteristic of disordered protein secondary structure, as has been previously observed and assigned for bR (Cladera et al., 1992; Taneva et al., 1995).

Fig. 2 A shows the absorbance change of the 1667-cm^{-1} band intensity as a function of temperature from 30 to 97°C. This gives a complete melting curve of bR in D_2O. It should be noted that at least two transitions are shown, a premelting transition ($T'_m \sim 76$°C) and the main transition ($T_m = 96$°C). It has been proposed that only the pretransition is reversible (Shnyrov and Mateo, 1993). Fig. 2 B shows the absorbance change of the 1623 cm^{-1} band under similar conditions as in Fig. 2 A. There is only one transition shown, i.e., the main transition with T_m of 96°C. This indicates that the band at 1623 cm^{-1} is associated with protein denaturation. Fig. 2, C and D show the change of absorbance at 1542 and 1436 cm^{-1}, respectively. The intensity changes are temperature dependent and no distinct T_m value can be found in the temperature range from 70 to 97°C. This reflects the H/D exchange behavior upon heating: the higher the temperature, the more the H/D exchange.

Our results agree with the previous finding that heating at temperatures up to 70°C hardly produces any change in the amide I and amide II bands in the FTIR spectra (Taneva et al., 1995), i.e., no bR secondary structure change observed, as shown previously in CD spectra (Shnyrov and Mateo, 1993). Because only the first transition is reversible (Shnyrov and Mateo, 1993), in the following sections, we focus on this transition by time-resolved FTIR study. The irreversibility of the melting transition at 96°C also prevents us from performing time-resolved studies of this transition.

Time-resolved FTIR study

Fig. 3 shows the time-resolved FTIR spectra in the region of 1800–1300 cm^{-1} obtained at different delay times as shown after the T-jump heating beam pulse. Delay times ranging from ns to ms are used. It can be seen that within $\sim$50 ns (trace (a)), the transient spectrum shows similar band features to that with small ΔT in Fig. 1 B with the amide I band shifting to lower frequency (from 1667 to 1651 cm^{-1}). Although the estimated T-jump reaches its maximum at approximately the same time as the heating pulse width, the T-jump induced conformation change is somewhat delayed. At $\sim$100 ns (trace (b)), the band changes from 1667 to 1651 cm^{-1} are significant, and the bands at 1542 and 1436 cm^{-1} (resulting from H/D exchange) begins to change. At $\sim$300
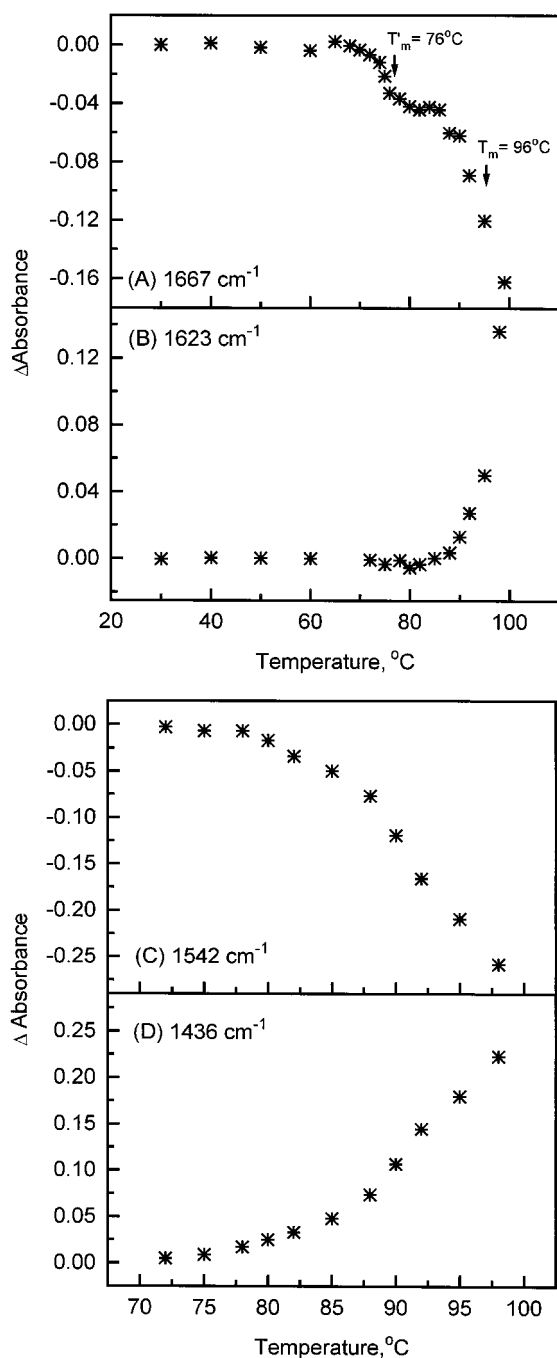
FIGURE 2 Absorbance changes at 1667 cm^{-1} (*A*), 1623 cm^{-1} (*B*), 1542 cm^{-1} (*C*), and 1436 cm^{-1} (*D*) as a function of temperature from 30 to 97°C (*A* and *B*) and from 70 to 97°C (*C* and *D*). The absorbance change in 1667 cm^{-1} serves as the melting curve of bR with a premelting transition (T'$_m$ = 76°C) and a main transition (T$_m$ = 96°C). The absorbance change at 1623 cm^{-1} shows the denaturing process that is associated with the main transition. *C* and *D* show the H/D exchange effect upon heating.
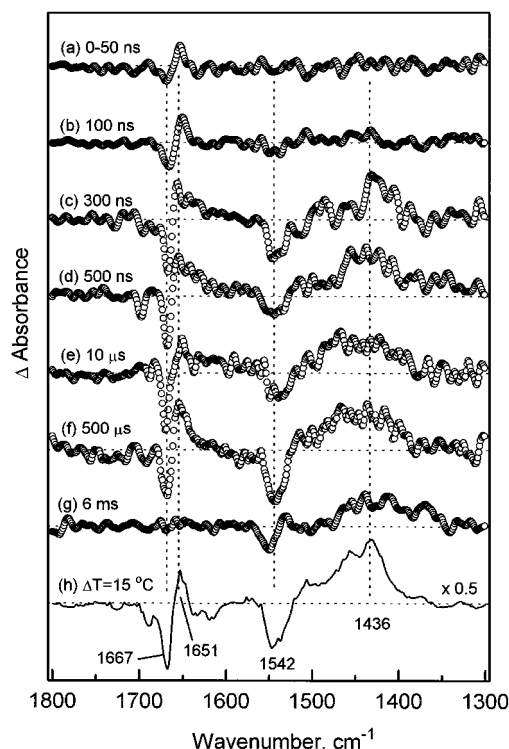

FIGURE 3 The time-resolved FTIR spectra obtained in the region of 1800–1300 cm^{-1} at different delay times after the T-jump pulse: 0–50 ns (*a*), 100 ns (*b*), 300 ns (*c*), 500 ns (*d*), 10 μs (*e*), 500 μs (*f*), 6 ms (*g*), and difference FTIR spectrum (*h*) (×0.5 of original spectrum with ΔT = 15°C shown in Fig. 1 *B*). These results show the change in the transient FTIR spectra upon a laser-induced T-jump. See detailed explanation in text.

ns (trace (c)), the spectral features (band shape, band position, and relative band area) become more or less equivalent to the difference FTIR spectrum with ΔT = 15°C (trace (h), T$_0$ = 72°C, taken from Fig. 2, ×0.5 of original). At ~6 ms (trace (g)), the transient spectrum shows a complete recov-

ery in the amide I band region. It should be noted that at 300–500 ns (traces (c) and (d)), two small bands are observed at ~1635 and ~1625 cm^{-1}. Within this time domain, the transient absorption bands in the region of 1651–1600 and 1530–1430 cm^{-1} change in a complex fashion as a result of the exposure of hydrophobic to aqueous medium (e.g., H-bonding breaking, solvent shifts, as well intensity enhancement). Our time-resolved FTIR results indicate that the transition from α_{II} to α_I occurs on the nanosecond time scale. In addition, from the correspondence of the transient spectrum obtained at certain time delays upon T-jump and the difference spectrum obtained at certain ΔT, a maximum ΔT of the T-jump is estimated as ~15°C (i.e., from 72 to ~87°C). The highest T-jump we use here is below the irreversible melting temperature T$_m$.

The transient absorption change of the amide I band of the α_I-helical feature at 1651 cm^{-1} during the T-jump is shown in Fig. 4. Fig. 4 *A* shows the rise curve of the α_I band intensity (obtained as an integral in the frequency region that covers the 1651 cm^{-1} band) in the nanosecond time region, which can be fitted to a double exponential function with apparent time constants of ~65 and 394 ns. This indicates that the structural change occurring in bR is relatively delayed with respect to the heating beam (pulse width 10 ns). We believe this is probably caused by the intrinsic
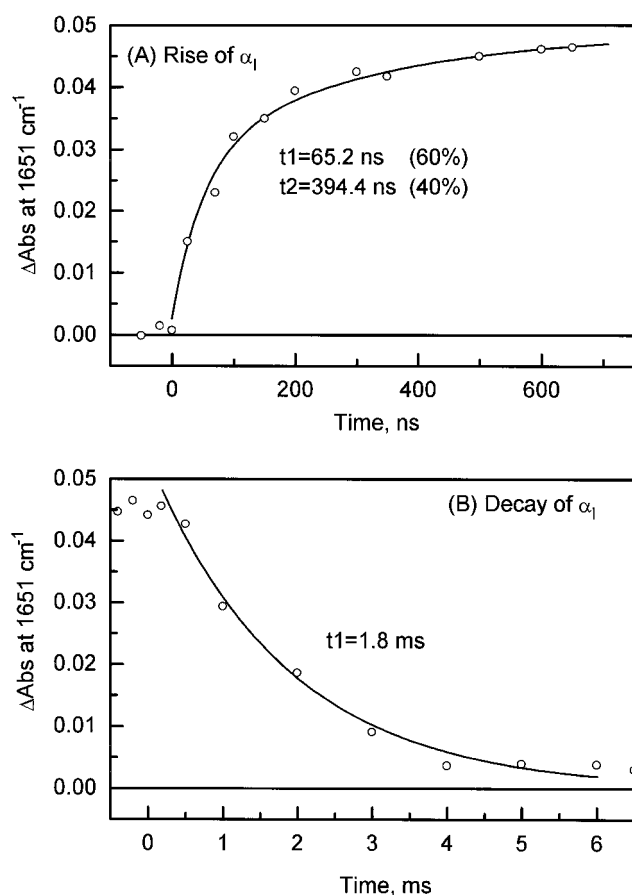
FIGURE 4   T-jump induced absorbance change at 1651 cm^{-1} as a function of time, obtained by integrating the transient band at 1651 cm^{-1}. (*A*) The rising process in nanosecond time range. (*B*) The decaying process in millisecond time range. The rising phase has two-exponential kinetics with rise times of 65 and 394 ns, indicating that two processes are involved in the transition from α_{II}-helix to α_I-helix structure. The decay phase shows single exponential kinetics with a lifetime ~1.8 ms.

properties of the α_{II} to α_I transitional behavior of bR. The structural recovery process is in the millisecond time range and can be fitted with a single exponential decay (lifetime ~1.8 ms, Fig. 4 *B*). This process is associated with the temperature decrease in bR suspension either as a direct result of the heat diffusion within milliseconds or because of the temperature-dependent kinetics of the back transition from α_I to α_{II}.

DISCUSSION

bR thermal stability

It has been shown that the melting temperature, T_m, changes in native bR as a function of pH (Kresheck et al., 1990) and that it changes from native bR to its various regenerated forms (Cladera et al., 1988; Kresheck et al., 1990). Two aspects are important for folding the seven α-helices in bR with its retinal chromophore: 1) hydrophobic interactions between the retinal and several residues, such as Trp (Cladera et al., 1992) and 2) a network of electrostatic

H-bond interactions around the protonated Schiff base and a few amino acid side chains such as Asp, Tyr, and Arg (Henderson et al., 1990; Otto et al., 1990). It seems that such H-bonding interactions are more significant than the hydrophobic interaction in stabilizing the bR structure (Cladera et al., 1992). The main transition of bR as revealed by DSC and IR spectra indicate the disruption of such H-bonding interactions.

The fully reversible pretransition occurring near 80°C has been attributed to structural reordering of the PM crystal lattice and is supported by the x-ray studies of Hiraki et al. (1981). This could also be related to the protein tertiary structure change that is reversible, as shown by the change in fluorescence emission within this temperature range (Shnyrov and Mateo, 1993). In our study, a secondary structural change is observed in this temperature range, i.e., an interconversion between α_{II}- and α_I-helical structures. From room temperature to higher, a slow color change from purple to reddish is observed (Hiraki et al., 1981), as indicated by the blue shift of λ_{max}. However, λ_{max} shows a sharp change at ~80°C (Jackson and Sturtevant, 1978; Hiraki et al., 1981). Shnyrov and Mateo (1993) believe that a molecular rearrangement (such as a decrease in the protein-lipid packing that allows for the exposure of some residues) occurs in this temperature range. That retinal is located across several helices, its color change suggests a change in the intrahelical geometry when increasing temperature. These two transitions and the secondary or tertiary structure change might be reflected in our time-resolved FTIR spectra. As shown in Fig. 4 *A*, the initial T-jump induced process has two components with rise times of 65 and 394 ns, respectively. A discussion of the processes to which these rise times might correspond is presented later.

Secondary structure of bR, interconversion between α_{II} and α_I, and premelting transition

The reason that bR has an α_{II}-helical instead of commonly found α_I-helical structure is still unknown. In addition, the intrinsic nature and the mechanism of the interconversion process between α_{II} and α_I is not yet understood. One possibility is that the proton pumping function of bR might be related to the weaker interhelical H-bonding interactions in α_{II}-helices. There are two aspects of conformational difference between the α_{II}- and α_I- helices proposed previously by Krimm and Dwivedi (1982), resulting from the difference in the ϕ and ψ dihedral angles in their α-helical conformation. First, that the C=O$\cdots$H-N H-bond length in α_{II} (N$\cdots$O distance is 3 Å) is slightly longer than that in α_I (N$\cdots$O = 2.86 Å), results in a slight weakening of the H-bond and therefore an increase in the C=O and N-H stretching force constants in α_{II}-helix. Second, α_{II} and α_I have different transition dipole coupling effects for two helices because of their structure difference. These two effects account for the observed frequency increase in amide I mode in α_{II} (Krimm and Dwivedi, 1982).

The vibrational band observed at 1651 cm^{-1} is located in the region of α_I-helices (Fraser and MacRae, 1973; Surewicz and Mantsch, 1988). The appearance of the 1651-cm^{-1} band occurs when the temperature increases from 72 to ~78°C (Fig. 1 *B*). This indicates that at temperatures lower than the main melting point, bR retains its helical structure. However, it undergoes a transition from α_{II}- to α_I-helices. Two transformations are expected to take place as ΔT increases: 1) C$=$O $\cdots$ H-N interhelical H-bond becomes stronger, because α_{II} is converted into α_I and 2) H/D exchange becomes faster and is temperature dependent, as observed when using D$_2$O as the solvent. This is reflected by the change in amide II band (Fig. 1 *B*). This work demonstrates that the membrane protein bR undergoes a fast secondary structural change from α_{II} to α_I upon T-jump, showing similar IR spectral features as that observed by the static difference spectra as temperature changes. However, from the present time-resolved study, it seems that these two transformations occur sequentially and not simultaneously, as discussed below.

Our time-resolved results in the present study reveal that the secondary structure changes occur during the so-called premelting transition (pretransition) at ~80°C, as reported by many authors, but concluded by using steady-state techniques (Jackson and Sturtevant, 1978; Brouillette et al., 1987; Cladera et al., 1988; Kresheck et al., 1990; Shnyrov et al., 1993). On the nanosecond time scale, two processes are resolved, one with a 65-ns apparent rise time and the other with a characteristic 394-ns rise time. These two rise times can be assigned to either two sequential processes, involving the changes in the protein structure, or assigned to one process occurring in two different parts of the protein because protein heterogeneity. The following experimental observations might support the first explanation. Fig. 3 shows that the changes of the band intensity of amide I and that at 1436 cm^{-1} (which monitors the H/D exchange) after the T-jump reveal different temporal behaviors. The intensity change of the 1436 cm^{-1} band begins on the ~100-ns time scale, whereas the amide I band intensity changes on the 0–50 ns time scale. These observations suggest that a fast intrahelical structure change from α_{II} to α_I occurs in the 65 ns. This leads to or is followed by the opening of the interhelical structure and the exposure of the hydrophobic portion of the protein occurring on the hundreds of ns time scales. This facilitates the observed increase in the H/D exchange. It is interesting that the amide I band at 1651 cm^{-1} decreases slightly in intensity and the new red shifted bands increase in intensity on the 100- to 500-ns time scale. The exposure of the hydrophobic part of the protein to aqueous medium could red shift the amide I band frequency and could be partly responsible for the change in the band shape in this region on this time scale. Also, the exposure of the hydrophobic part of the protein leads a complex and time-dependent band shape changes on the high frequency side of the 1436-cm^{-1} band. The origin of these changes cannot be assigned at this time.

REFERENCES

Arrondo, J. R., J. Castresana, J. M. Valpuesta, and F. M. Goni. 1994. Structure and thermal denaturation of crystalline and noncrystalline cytochrome oxides as studied by infrared spectroscopy. *Biochemistry.* 33:11650–11655.

Ballew, R. M., J. Sabelko, and M. Gruelebe. 1996. Direct observation of fast protein folding: the initial collapse of apomyoglobin. *Proc. Natl. Acad. Sci. USA.* 93:5759–5764.

Birge, R. R. 1990. Photophysics and molecular electronic applications of the rhodopsins. *Annu. Rev. Phys. Chem.* 41:683–733.

Brouillette, C. G., D. D. Muccio, and T. K. Finney. 1987. pH dependence of bacteriorhodopsin thermal unfolding. *Biochemistry.* 26:7431–7438.

Cladera, J., M. L. Galisteo, M. Dunach, P. L. Mateo, and E. Padros. 1988. Thermal denaturation of deionized and native purple membrane. *Biochim. Biophys. Acta.* 943:148–156.

Cladera, J., M. L. Galisteo, M. Sabes, P. L. Mateo, and E. Padros. 1992. The role of retinal in the thermal stability of the purple membrane. *Eur. J. Biochem.* 207:581–585.

Ebrey, T. G. 1993. Light energy transduction in bacteriorhodopsin. *In* Thermodynamics of Membrane Receptors and Channels. M. B. Jackson, editor. CRC Press, Boca Raton, FL. 353–387.

Fraser, R. D. B., and T. P. MacRae. 1973. Conformation of Fibrous Proteins and Related Synthetic Polypeptides, Chapter 5. Academic Press, New York. 95–125.

Gibson, N. J., and J. Y. Cassim. 1989. Evidence for an α_{II}-type helical conformation for bacteriorhodopsin in the purple membrane. *Biochemistry.* 28:2134–2139.

Henderson, R., J. M. Baldwin, T. A. Ceska, F. Zemlin, E. Beckmann, and K. H. Dowing. 1990. Model for the structure of bacteriorhodopsin based on high-resolution electron cryo-microscopy. *J. Mol. Biol.* 213:899–929.

Hiraki, K., T. Hamanaka, T. Mitsui, and Y. Kito. 1981. Phase transitions of the purple membrane and the brown holo-membrane: x-ray diffraction, circular dichroism spectrum and absorption spectrum studies. *Biochim. Biophys. Acta.* 647:18–28.

Jackson, M. B., and J. M. Sturtevant. 1978. Phase transition of the purple membranes of *Halobacterium halobium. Biochemistry.* 17:911–915.

Kresheck, G. C., C. T. Lin, L. N. Williamson, W. R. Mason, D.-J. Jang, and M. A. El-Sayed. 1990. The thermal stability of native, delipidated, deionized and regenerated bacteriorhodopsin. *J. Photochem. Photobiol. B: Biol.* 7:289–302.

Krimm S., and A. M. Dwivedi. 1982. Infrared spectrum of the purple membrane: clue to a proton conduction mechanism. *Science.* 216:407–408.

Lanyi, J. K. 1993. Proton translocation mechanism and energetics in the light-driven pump bacteriorhodopsin. *Biochim. Biophys. Acta.* 1183:241–261.

Mathies, R. A., S. W. Lin, J. B. Ames, and W. T. Pollard. 1991. From femtosecond to biology: mechanism of bacteriorhodopsin's light-driven proton pump. *Annu. Rev. Biophys. Biophys. Chem.* 20:491–518.

Oesterhelt, D., and W. Stoeckenius. 1974. Isolation of the cell membrane of *Halobacterium halobium* and its fractionation into red and purple membrane. *Methods Enzymol.* 31:667–678.

Otto, H., T. Marti, M. Holz, T. Mogi, L. J. Stern, F. Engel, H. G. Khorana, and M. P. Heyn. 1990. Substitution of amino acids Asp-85, Asp-212, and Arg-82 in bacteriorhodopsin affects the proton release phase of the pump and the pK of the Schiff base. *Proc. Natl. Acad. Sci. USA.* 87:1018–1022.

Phillips, C. M., Y. Mizutani, and R. M. Hochstrasser. 1995. Ultrafast thermally induced unfolding of Rnase A. *Proc. Nat. Acad. Sci. USA.* 92:7292–7296.

Shnyrov, V. L., and P. L. Mateo. 1993. Thermal transition in the purple membrane from *Halobacterium halobium. FEBS Lett.* 324:237–240.

Surewicz, W. K., and H. H. Mantsch. 1988. New insight into protein secondary structure from resolution-enhanced infrared spectra. *Biochim. Biophys. Acta.* 952:115–130.

Taneva, S. G., J. M. M. Caaveiro, A. Muga, and F. M. Goni. 1995. A pathway for the thermal destabilization of bacteriorhodopsin. *FEBS Lett.* 367:297–300.

Torres, J., F. Sepulcre, and E. Padros. 1995. Conformational changes in bacteriorhodopsin associated with protein-protein interactions: a functional α_I-α_{II} helix switch? *Biochemistry.* 34:16320–16326.

Tuzi, S., A. Naito, and H. Saito. 1994. ^{13}C NMR study on conformation, and dynamics of the transmembrane α-helices, loops, and C-terminus of [3-^{13}C] Ala-labeled bacteriorhodopsin. *Biochemistry.* 33:15046–15052.

Vogel, H., and W. Gartner. 1987. The secondary structure of bacteriorhodopsin determined by Raman and circular dichroism spectroscopy. *J. Biol. Chem.* 262:11464–11469.

Williams, S., T. P. Causgrove, R. Gilmanshin, K. S. Fang, R. H. Callender, W. H. Woodruff, and R. B. Dyer. 1996. Fast events in protein folding: helix melting and formation in a small peptide. *Biochemistry.* 35:691–697.